Robust Adaptive Variable Structure Control of Spacecraft Under Control Input Saturation

Jovan D. Bošković,[*] Sai-Ming Li,[†] and Raman K. Mehra[‡]
Scientific Systems Company, Inc., Woburn, Massachusetts 01801

In this paper we propose two globally stable control algorithms for robust stabilization of spacecraft in the presence of control input saturation, parametric uncertainty, and external disturbances. The control algorithms are based on variable structure control design and have the following properties: 1) fast and accurate response in the presence of bounded external disturbances and parametric uncertainty; 2) explicit accounting for control input saturation; 3) computational simplicity and straightforward tuning. We include a detailed stability analysis for the resulting closed-loop system. The stability proof is based on a Lyapunov-like analysis and the properties of the quaternion representation of spacecraft dynamics. It is also shown that an adaptive version of the proposed controller results in substantially simpler stability analysis and improved overall response. We also include numerical simulations to illustrate the spacecraft performance obtained using the proposed controllers.

I. Introduction

FUTURE spacecraft will be expected to achieve highly accurate pointing, fast slewing, and other fast maneuvers from large initial conditions and in the presence of large environmental disturbances, measurement noise, large uncertainties, subsystem and component failures, and control input saturation. Additional requirements to the spacecraft control systems will be imposed by a newly developed concept of coordinated control of multiple spacecraft (see, for instance, Refs. 1 and 2). In the latter case multiple spacecraft will be used for tasks that are presently not possible to achieve with a single spacecraft. Coordinated control of such spacecraft formations imposes stringent requirements on the control of each spacecraft because the formation objectives can be achieved efficiently only when all individual spacecraft are tightly controlled to respond rapidly and accurately to the formation coordination commands. This should be the case even in the presence of failures, uncertainties, and disturbances.

The design of such control systems for a single spacecraft is a complex task as a result of coupled nonlinear attitude dynamics and attached flexible structures.[3] In addition, minimal representation of attitude dynamics, such as Euler angles or Rodrigues parameters,[4] contain singularities and are hence not well suited for the design of global control algorithms. For this reason nonlinear tracking control algorithms based on global representation of spacecraft dynamics, such as that employing quaternions,[4] are needed to ensure that the control objectives are met over a large range of operating conditions. Our literature search has revealed that there are essentially two classes of such algorithms: 1) the algorithms based on a mixed term in a Lyapunov-like function for the closed-loop system, such as those from Ref. 5, and 2) the algorithms based on a suitable coordinate transformation and Lyapunov-like analysis, such as those from Ref. 6.

Spacecraft commonly operate in the presence of various disturbances, including gravitational torque, aerodynamic torque, radiation torque, and other environmental and nonenvironmental torques. The problem of disturbance rejection is particularly pronounced in the case of low-Earth-orbiting satellites that operate in the altitude ranges where their dynamics is substantially affected by most of the preceding disturbances. In addition, as the inertia matrix of spacecraft is usually not known exactly, spacecraft control design needs also take parametric uncertainty into account. Hence disturbance rejection control strategies that are also robust to parametric uncertainty are of great interest.

Another important problem encountered in practice is that of control input saturation. As it is well known, in the case of control algorithms with integral terms control input saturation can cause the so-called integrator windup when the integral of the stabilization or tracking error accumulates over time and hence prevents the control input from unsaturating. This can lead to substantial performance deterioration and even to instability of the system. Hence globally stable tracking algorithms that take control input saturation explicitly into account are of interest in practice. Such control algorithms are of particular interest in spacecraft control where the control objectives are to be achieved with limited control authority. In Ref. 7 the authors considered this problem using the equivalent control approach. The control design was found to be effective in simulation studies. However, the stability analysis when the input is saturated was lacking.

The main contribution of this paper is the design of a class of globally stable control algorithms for spacecraft stabilization that take into account control input saturation explicitly, assure fast and accurate response, and achieve effective compensation for the effect of external disturbances and parametric uncertainty. In addition, the proposed algorithms are computationally simple and involve straightforward tuning. Their design is based on the variable structure approach to control systems design.

The paper is organized as follows: Sec. II contains an overview of the sliding mode control design and its application to spacecraft control. In Sec. III we state the control problem for a spacecraft in the presence of bounded disturbances, parametric uncertainty, and control input saturation. Section IV describes the properties of the equivalent control-based sliding mode control design for spacecraft. Sections V and VI contain a detailed description of two globally stable control algorithms and the proof of stability for the resulting closed-loop system, whereas Sec. VII presents simulation examples of the proposed control algorithms on a generic spacecraft model.

II. Variable Structure and Sliding Mode-Based Control of Spacecraft

The main idea behind the variable structure control approach is to design suitable algorithms for changing the structure of the control system during its course of operation to exploit the desirable features of different structures. Under certain conditions a new behavior, known as sliding mode, can arise in such systems as a result of infinitely frequent switching between different structures. The method was first proposed by Emelyanov in the early 1950s and elaborated by his group and a number of other researchers.[8−11]

*Senior Research Engineer, 500 W. Cummings Park, Suite 3000. Member AIAA.
†Research Engineer, 500 W. Cummings Park, Suite 3000.
‡President and CEO, 500 W. Cummings Park, Suite 3000. Member AIAA.

Sliding mode can occur under certain conditions in a dynamical system with discontinuous inputs. Such inputs can force the solutions of the system to a hypersurface in the state space where the behavior of the system is dominated by lower-order dynamics and is invariant to external disturbances and parameter variations. In the case when the existence of a sliding mode cannot be guaranteed, the discontinuous controller is referred to as the Variable Structure Control (VSC) algorithm. The use of both sliding mode and variable structure controllers also results in finite time response. These properties have been extensively used to design highly robust tracking controllers for both linear and nonlinear systems and have been applied to a wide variety of engineering systems.[10,11]

Because the variable structure controllers use high-frequency switching to achieve the objective of maintaining the solutions of the system on the sliding surface and because of the imperfection of the switching devices, chattering of the signals in the system occurs in practice. This undesirable feature needs to be removed by replacing the sign functions commonly used to implement such controllers by either the saturation function,[10] or by an approximate sign function.[12−14] This action results in the solutions of the closed-loop system being confined to a boundary layer around the switching surface rather than to the surface itself so that the tracking error remains bounded rather than converging to zero. The size of the resulting set of uniform ultimate boundedness can be adjusted with the proper choice of the free design parameters.

VSC has been used for spacecraft attitude control by a number of authors. Singh and Iyer,[15] Dwyer and Sira-Ramirez,[16] and Crassidis and Markley[17] developed nonglobal VSC algorithms for minimal attitude representation such as Euler angles and Rodrigues parameters. Among those based on attitude representation using quaternions, the algorithms developed by Lo and Chen[18] and McDuffie and Shtessel[19] are not global because the reciprocal of one of the quaternions is used to implement the control law. Vadali[20] was the first to develop a global VSC algorithm for attitude control. The sliding surface is determined by the use of optimal control theory for a specific performance index. However, the analysis appears incomplete as the nonlinear attitude dynamics is neglected. Recently, Terui[21] extended this approach to include translational dynamics of the spacecraft as well. Most of the work just mentioned uses the so-called equivalent control component in the control law to keep the system dynamics on the sliding surface. None of them addresses the problem of control input saturation explicitly.

In this paper we will develop several algorithms for global stabilization of spacecraft attitude dynamics. The algorithms are based on variable structure control and take into account the control input saturation explicitly. We will also show that such algorithms ensure fast and accurate response and are highly robust to external disturbances and parametric uncertainty. This is discussed in the following sections.

III.   Problem Statement

In this section we state the problem of spacecraft stabilization in the presence of bounded disturbances, parametric uncertainty and control input saturation.

Spacecraft Attitude Dynamics

The spacecraft is assumed to be a rigid body with actuators that provide torques about three mutually perpendicular axes that define a body-fixed frame $\mathcal{B}$. The equations of motion are given by (see Ref. 4)

$$J\dot{\Omega} = -\Omega^{\times}J\Omega + \text{sat}(u) + z \tag{1}$$

$$\dot{\epsilon} = \tfrac{1}{2}(\epsilon^{\times} + \epsilon_0 I)\Omega \tag{2}$$

$$\dot{\epsilon}_0 = -\tfrac{1}{2}\epsilon^T\Omega \tag{3}$$

where $\Omega \in \mathbb{R}^3$ denotes the inertial angular velocity of the spacecraft with respect to an inertial frame $\mathcal{I}$, $J = J^T$ denotes the positive definite inertia matrix of the spacecraft, $\epsilon \in \mathbb{R}^3$ and $\epsilon_0 \in \mathbb{R}$ denote the Euler parameters (quaternions) that represent the orientation of $\mathcal{B}$ with respect to the inertial frame $\mathcal{I}$ and satisfy the constraint $\epsilon^T\epsilon + \epsilon_0^2 = 1$, and I denotes a 3×3 identity matrix. Further, $u \in \mathbb{R}^3$ denotes the vector of control torques commanded by the controller,

and $\text{sat}(u) = [\text{sat}(u_1)\ \text{sat}(u_2)\ \text{sat}(u_3)]^T$ is the vector of actual control torques generated by the actuators (or thrusters), where $\text{sat}(u_i)$ denotes the nonlinear saturation characteristic of the actuators and is of the form

$$\text{sat}(u_i) = \begin{cases} u_{mi}, & u_i > u_{mi} \\ u_i & -u_{mi} \leq u_i \leq u_{mi} \\ -u_{mi}, & u_i < -u_{mi} \end{cases} \tag{4}$$

The notation $a^{\times}$ for a vector $a = [a_1\ a_2\ a_3]^T$ is used to denote the skew-symmetric matrix

$$a^{\times} = \begin{bmatrix} 0 & -a_3 & a_2 \\ a_3 & 0 & -a_1 \\ -a_2 & a_1 & 0 \end{bmatrix}$$

Disturbances and Control Inputs

In Eq. (1), $z \in \mathbb{R}^3$ denotes a vector of external disturbances. These include environmental torques such as gravitational torque and torque as a result of aerodynamic drag, solar radiation, and magnetic effects. We will assume that $z(t) \in \mathcal{S}_z = \{z : \|z\| \leq \bar{z}\}$ for all time, where the upper bounds $\bar{z}$ on the magnitude of the disturbance is known. In addition, because the total control authority is limited, we define a set $\mathcal{S}_u = \{u : -u_{mi} \leq u_i \leq u_{mi}, i = 1, 2, 3\}$, such that $u \in \mathcal{S}_u$ implies that $\text{sat}(u) \equiv u$. For simplicity, we shall assume that all three control input torques have the same bound, i.e., $u_{mi} = \bar{u}_m$. The relationship between u_m and $\bar{z}$ is addressed in the following assumption:

Assumption 1:

$$\bar{u}_m > \bar{z}$$

Loosely speaking, the assumption essentially states that the available control authority is sufficient to reject any disturbances from $\mathcal{S}_z$, which is a reasonable assumption in practice. Let $\bar{\lambda}_J$ and $\underline{\lambda}_J$ denote known upper and lower bounds on the norm of the inertia matrix J, respectively. The control objective is now stated as follows:

Control Objective: For the plant (1–3), under assumption 1, design a control input $u(t)$ that belongs to $\mathcal{S}_u$ for all time; for all physically realizable initial conditions, all $z \in \mathcal{S}_z$, and all $J = J^T > 0$ (such that $\underline{\lambda}_J \leq \|J\| \leq \bar{\lambda}_J$); and ensures that $\lim_{t \to \infty} \Omega(t) = \lim_{t \to \infty} \epsilon(t) = 0$.

In this paper we will use VSC to achieve the preceding control objective. We will first describe an approach to sliding mode control design for spacecraft based on equivalent control and then propose two global stabilization algorithms that achieve disturbance rejection in the presence of parametric uncertainty and control input saturation.

IV.   Equivalent Control-Based Sliding Mode Control Design for Spacecraft

In this section, based on the existing results on sliding mode control,[9,10] we will present the design procedure for such controllers for spacecraft. The approach generally assumes unlimited control authority, and hence $\text{sat}(u) \equiv u$ in Eq. (1). For the sake of simplicity, we shall assume that $z \equiv 0$ in this section.

Sliding Surface

In the context of spacecraft control, the equivalent control-based sliding mode control design is based on the use of the following sliding surface:

$$s = \Omega + k\epsilon \tag{5}$$

where $k > 0$ is a scalar.

Equivalent Control-Based Sliding Mode Controller

After premultiplying Eq. (5) by J, differentiating it with respect to time, and using Eqs. (1) and (2), we obtain

$$J\dot{s} = -\Omega^{\times}J\Omega + u + \tfrac{1}{2}kJ(\epsilon^{\times} + \epsilon_0 I)\Omega \tag{6}$$

The control input is chosen in the form

$$u = u_{\text{eq}} + u_{\text{vs}} \tag{7}$$

where u_{eq} denotes the equivalent control component[9] and is chosen to ensure that $\dot{s}(t) = 0$ for all time, i.e.,

$$u_{\text{eq}} = \Omega^{\times} J\Omega - \tfrac{1}{2}kJ\left(\epsilon^{\times} + \epsilon_0 I\right)\Omega \qquad (8)$$

The preceding control law can be augmented with feedback terms in Ω and ϵ, as suggested in Ref. 7. Control law (7) also contains u_{vs}, the variable structure component. This component is to be chosen to ensure that the sliding surface $s = 0$ is attractive and can be reached in finite time, as shown next.

Stability Analysis

Consider a scalar function of the form

$$V(s) = \tfrac{1}{2}s^T J s$$

Using Eqs. (5–8), the first derivative of V along the motions of the system yields

$$\dot{V}(s) = s^T u_{\text{vs}}$$

By choosing

$$u_{\text{vs}} = -\Sigma(s)\,\alpha$$

where

$$\alpha = [\alpha_1 \quad \alpha_2 \quad \alpha_3]^T, \qquad \alpha_i > 0$$

$$\Sigma(s) \triangleq \text{diag}\{\text{sgn}(s_1) \quad \text{sgn}(s_2) \quad \text{sgn}(s_3)\}$$

and $\text{sgn}(\cdot)$ denotes the sign function, i.e.,

$$\text{sgn}(\psi) = \begin{cases} 1, & \psi > 0 \\ 0, & \psi = 0 \\ -1, & \psi < 0 \end{cases}$$

we obtain

$$\dot{V}(s) = -\sum_{i=1}^{3}\alpha_i|s_i| < 0$$

Hence, V is the Lyapunov function in the s-space. It follows that $s \in \mathcal{L}^{\infty}$ and $\lim_{t \to \infty} s(t) = 0$.

Speed of Response

Let $\bar{\alpha} = \min\{\alpha_i\}$. To show that $s = 0$ is achieved in finite time from any initial condition $s(0) = s_0$, we further use the fact that

$$\sum_{i=1}^{3}|s_i| \geq \|s\|$$

(where $\|\cdot\|$ denotes the Euclidean norm), and the definition of $V(s)$ to obtain $V(s) \leq \tfrac{1}{2}\bar{\lambda}_J\|s\|^2$ (where $\bar{\lambda}_J$ denotes the maximum eigenvalue of the inertia matrix J). Then we have

$$\dot{V}(s) \leq -\bar{\alpha}\|s\| \leq -\left(\sqrt{2}\bar{\alpha}/\sqrt{\bar{\lambda}_J}\right)\sqrt{V}$$

Because $V[s(t)] > 0$ for all $s(t) \neq 0$, we can use the comparison principle[22] and integrate the preceding differential inequality to obtain

$$V[s(t)] \leq \left\{\sqrt{V[s(0)]} - \left(\sqrt{2}\bar{\alpha}/2\sqrt{\bar{\lambda}_J}\right)t\right\}^2$$

Because $V(s) \geq \tfrac{1}{2}\underline{\lambda}_J\|s\|^2$, where $\underline{\lambda}_J$ is the minimum eigenvalue of J, we have

$$\|s(t)\| \leq \left(1/\sqrt{\underline{\lambda}_J}\right)\left\{\sqrt{2V[s(0)]} - \left(\bar{\alpha}/\sqrt{\bar{\lambda}_J}\right)t\right\}$$

$$\leq \left(1/\sqrt{\underline{\lambda}_J}\right)\left[\sqrt{\bar{\lambda}_J}\|s_0\| - \left(\bar{\alpha}/\sqrt{\bar{\lambda}_J}\right)t\right]$$

where $s_0 = s(0)$. Hence the sliding surface $s = 0$ is reached from any initial condition at or before time instant

$$t_f = (\bar{\lambda}_J/\bar{\alpha})\|s_0\|$$

Dynamics on the Sliding Surface

To determine the spacecraft dynamics on the sliding surface, we will use an approach similar to that from Ref. 20. Once $s = 0$ is reached, because u_{eq} ensures that $\dot{s}(t) = 0$ for all time, the motions of the system will remain on the sliding surface for all time. Hence the spacecraft dynamics on the sliding surface (also referred to as the sliding mode or sliding regime) can be obtained by solving $s = 0$ for Ω [using Eq. (5)] and substituting into Eqs. (2) and (3). This yields

$$\dot{\epsilon} = -\tfrac{1}{2}k\left(\epsilon^{\times} + \epsilon_0\right)\epsilon = -\tfrac{1}{2}k\epsilon_0\epsilon \qquad (9)$$

$$\dot{\epsilon}_0 = -\tfrac{1}{2}\epsilon^T(-k\epsilon) = (k/2)\left(1 - \epsilon_0^2\right) \qquad (10)$$

Let t_s be the time instant when the sliding mode is reached. Upon integrating the last equation, we obtain

$$\epsilon_0(t) = 1 - \frac{2[1 - \epsilon_0(t_s)]e^{-k(t-t_s)}}{1 + \epsilon_0(t_s) + [1 - \epsilon_0(t_s)]e^{-k(t-t_s)}} \qquad t \geq t_s \quad (11)$$

Hence $\lim_{t \to \infty} \epsilon_0(t) = 1$. Because $\epsilon^T\epsilon + \epsilon_0^2 = 1$ and $\Omega = -k\epsilon$ on the sliding surface, we also have

$$\lim_{t \to \infty}\|\epsilon(t)\| = \lim_{t \to \infty}\|\Omega(t)\| = 0$$

Comments

1) One of the major problems related to the preceding control law is that of input chattering, which arises as a result of imperfections of available switching devices. Hence the sign function is commonly replaced by either the saturation function or an approximate sign function. In such a case we can only guarantee that the output error will converge to a small set around the origin, rather than to zero.

2) Another problem associated with most of the global control algorithms for spacecraft is caused by the quaternion representation of its orientation. As it is well known (see, e.g., Ref. 4), $\epsilon_0 = 1$ and $\epsilon_0 = -1$ represent the same orientation. Because the preceding control law guarantees that $\lim_{t \to \infty} \epsilon_0(t) = 1$, this implies that, even for small deviations from $\epsilon_0(0) = -1$, the spacecraft will execute a full rotation in order to arrive at the point $\epsilon_0 = 1$ (that coincides with the point $\epsilon_0 = -1$). This can be prevented by using an approach similar to that from Ref. 20. In such a case the sliding surface is modified as $s = \Omega + k\epsilon\,\text{sgn}(\epsilon_0)$. Then, in the sliding regime we have from Eq. (10) that $\dot{\epsilon}_0 = -\tfrac{1}{2}\epsilon^T[-k\epsilon\,\text{sgn}(\epsilon_0)] = (k/2)(1 - \epsilon_0^2)\,\text{sgn}(\epsilon_0)$. This implies that, for $\epsilon_0(0) > 0$, $\lim_{t \to \infty} \epsilon_0(t) = 1$, and for $\epsilon_0(0) < 0$, $\lim_{t \to \infty} \epsilon_0(t) = -1$.

3) Another important problem associated with the preceding control law is that it does not take the control input saturation explicitly into account. This is clear from the expression (8) as $u_{\text{eq}}(t)$ depends on the instantaneous response of the system.

Hence, in this paper we propose two global stabilization algorithms that retain favorable properties of the sliding mode controllers and, in addition, achieve the control objective with the available control authority. This is discussed in the following sections.

V. Sliding Mode Control Under Control Input Saturation

In this section we propose a sliding mode control law for the system (1–3), which ensures that $u(t) \in \mathcal{S}_u$ for all time and, in addition, that the spacecraft stabilization is achieved for all $z \in \mathcal{S}_z$ and all $J = J^T > 0$, where $\underline{\lambda}_J \leq \|J\| \leq \bar{\lambda}_J$, and $\underline{\lambda}_J, \bar{\lambda}_J$ are known. To motivate the design of the proposed control law, we will first consider a simpler control objective of stabilization of Ω only. This problem was studied in Ref. 7. Hence we focus only on Eq. (1) and consider a Lyapunov function candidate $V(\Omega) = \tfrac{1}{2}\Omega^T J\Omega$. Its first derivative along the solutions of Eq. (1) yields

$$\dot{V}(\Omega) = \Omega^T u + \Omega^T z$$

If we use the VSC law of the form

$$u = -\Sigma(\Omega)u_m \qquad (12)$$

where

$$\Sigma(\Omega) \triangleq \mathrm{diag}[\mathrm{sgn}(\Omega_1) \quad \mathrm{sgn}(\Omega_2) \quad \mathrm{sgn}(\Omega_3)]$$

$$u_m = [\bar{u}_m \quad \bar{u}_m \quad \bar{u}_m]^T$$

we obtain

$$\dot{V}(\Omega) \leq -\bar{u}_m \sum_{i=1}^{3} |\Omega_i| + \|\Omega\|\bar{z} \quad (\text{because } \|z\| < \bar{z})$$

$$\leq -(\bar{u}_m - \bar{z})\|\Omega\| \quad \left(\text{because } \sum_{i=1}^{3} |\Omega_i| \geq \|\Omega\|\right)$$

$$< 0$$

From Assumption 1, we have $\bar{u}_m > \bar{z}$. From the Lyapunov second method we now obtain that $\Omega \in \mathcal{L}^\infty$ and $\lim_{t \to \infty} \Omega(t) = 0$. Furthermore, because $V(\Omega) \leq \frac{1}{2}\bar{\lambda}_J\|\Omega\|^2$, it follows that $\dot{V}(t) \leq -\alpha\sqrt{[V(t)]}$ for some $\alpha > 0$. By using the comparison principle[22] as in the case of the sliding mode control described in the preceding section, it can be shown that $\Omega(t)$ converges to zero in finite time. An important point here is that global stabilization of $\Omega(t)$ is achieved despite the presence of a bounded disturbance z and with the available control authority because from Eq. (12) it is clear that $u(t) \in \mathcal{S}_u$ for all time.

Because our objective is to stabilize both $\Omega(t)$ and $\epsilon(t)$, a question that arises in this context is whether a control law similar to $u = -\Sigma(\Omega)u_m$ can be found to achieve this objective.

We recall that the analysis from Sec. IV has revealed that in the case of equivalent control-based sliding mode controller design the dynamics of a spacecraft on the sliding surface [Eq. (5)] is obtained when $s = 0$ and results in $\lim_{t \to \infty} \Omega(t) = \lim_{t \to \infty} \epsilon(t) = 0$. We also recall that the variable structure component u_{vs} of the control law (7) is a function of s only and ensures that the sliding surface $s = 0$ is reached in finite time. We hence propose a control law that consists only of the variable structure component and is of the form

$$u = -\Sigma(s)u_m \qquad (13)$$

where $\Sigma(s) \triangleq \mathrm{diag}[\mathrm{sgn}(s_1) \ \mathrm{sgn}(s_2) \ \mathrm{sgn}(s_3)]$. Hence this control law ensures that $u(t) \in \mathcal{S}_u$ for all time. Although this control law is practically appealing because of its simplicity, a question arises whether it is possible to find conditions under which it achieves the objective of global stabilization of both Ω and ϵ in the case when $z \in \mathcal{S}_z$, and for all $J = J^T > 0$, when $\underline{\lambda}_J \leq \|J\| \leq \bar{\lambda}_J$. Our analysis revealed that this is the case if a condition is imposed on the gain k in Eq. (5). This condition is relatively benign because it does not affect the magnitude of the control input and is summarized in the following theorem:

Theorem 1: Let the overall system be given by Eqs. (1–3), (5), and (13). For any β such that $0 < \beta < 1$, if $\bar{u}_m > \bar{z}/\beta$ and the gain k from Eq. (5) satisfies

$$k < \sqrt{(1-\beta)(\bar{u}_m - \bar{z})\underline{\lambda}_J \mid 6\bar{\lambda}_J^2} \qquad (14)$$

then $\Omega(t)$ is bounded and $\lim_{t \to \infty} \Omega(t) = \lim_{t \to \infty} \epsilon(t) = 0$ for all $z \in \mathcal{S}_z$ and all $J = J^T > 0$ such that $\underline{\lambda}_J \leq \|J\| < \bar{\lambda}_J$.

The proof of this theorem is based on the properties of the sliding model control law and the quaternion representation of the spacecraft dynamics. These properties are summarized in the following assertion.

Assertion 1:

1) If $|\Omega_i| > k$, then $\mathrm{sgn}(\Omega_i) = \mathrm{sgn}(s_i)$.
2) For all Ω_i, $\Omega_i \, \mathrm{sgn}(s_i) \geq |\Omega_i| - 2k$.

Proof of Assertion 1:

1) Because $s_i = \Omega_i + k\epsilon_i$ and $|\epsilon_i| \leq 1$, statement 1) follows. This is illustrated in Fig. 1. It is seen that $\mathrm{sgn}(\Omega_i) = -\mathrm{sgn}(s_i)$ only in the shaded area in the figure. Hence the condition of statement 1)
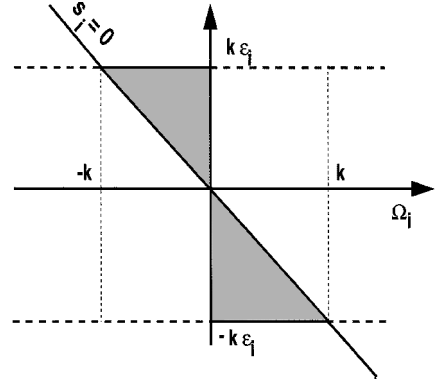

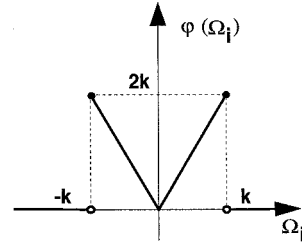
Fig. 1   Proof of statement 1) of Assertion 1.

Fig. 2   Proof of statement 2) of Assertion 1.

of Assertion 1 is conservative because $\mathrm{sgn}(\Omega_i) = \mathrm{sgn}(s_i)$ even if $|\Omega_i| < k$ and is inside the set

$$\mathcal{X}_i \triangleq \{(\Omega_i, \epsilon_i) : \Omega_i \geq 0, \Omega_i \geq -k\epsilon_i \ \text{ or } \ \Omega_i \leq 0, \Omega_i \leq -k\epsilon_i\} \qquad (15)$$

However, for the proof of Theorem 1 we will focus on the sets $\mathcal{S}_i \triangleq \{\Omega_i : |\Omega_i| < k\}$. It is clear that the condition in statement 1) of Assertion 1 is independent of ϵ_i and is satisfied for all $\Omega_i \in \mathcal{S}_i^c$, where the sets $\mathcal{S}_i^c$ denote the complements of $\mathcal{S}_i$.

2) Let $\varphi(\Omega_i) \triangleq \max_{|\epsilon_i| \leq 1}\{|\Omega_i| - \Omega_i \, \mathrm{sgn}(s_i)\}$. This function is shown in Fig. 2. It is clear from the figure that $\varphi(\Omega_i) \leq 2k$. Hence statement 2) of Assertion 1 follows. $\square$

Proof of Theorem 1: The proof of the theorem is fairly involved and consists of three main steps. We will outline these steps next, and a more detailed analysis will be given in the Appendix. The main idea behind the proof is to demonstrate the following:

Step 1: Any motion of the overall system that starts from an arbitrary initial condition is either inside or enters a closed compact subset of the state space containing the origin in finite time.

Step 2: For all motions inside this subset, there exists a value of k for which the sliding surface $s = 0$ is attractive.

Step 3: Once on the sliding surface, $\Omega(t)$ and $\epsilon(t)$ tend to zero. In addition, this is achieved for any $z \in \mathcal{S}_z$, and for any $J = J^T > 0$ such that $\underline{\lambda}_J \leq \|J\| \leq \bar{\lambda}_J$.

These steps are described in detail in the Appendix. $\square$

Based on the results just presented, the following comments are in order:

1) Because the control law (13) ensures that $u(t) \in \mathcal{S}_u$ for all time, Theorem 1 essentially states that the control objective will be achieved not only with the available control authority, but also in the presence of bounded disturbances and uncertainty in J. This, along with its simplicity, is the main feature of the control law (13).

2) To avoid chattering of control input, the sign function in the control law (13) can be replaced by an approximate sign function of the form $f(\psi) = \psi/(|\psi| + \delta)$, where $\delta > 0$ is constant and is commonly chosen to be sufficiently small. The control law then becomes

$$u = -\tilde{\Sigma}(s)u_m \qquad (16)$$

where $\tilde{\Sigma}(s) \triangleq \mathrm{diag}[s_1/(|s_1| + \delta) \ s_2/(|s_2| + \delta) \ s_3/(|s_3| + \delta)]$. In this case it can be shown that $\Omega(t)$ and $\epsilon(t)$ tend asymptotically to a small set around the origin. This can be proved along the same lines as in the case of the sign function and will not be included. Simulation examples will be included in Sec. VII to demonstrate the efficacy of this control law.

3) The main drawbacks of the preceding control law are the following: a) the condition (14) can be fairly restrictive. Because k is used to achieve relative weighting between $\Omega(t)$ and $\epsilon(t)$, a small k can result in a slow response in $\epsilon(t)$. b) It is seen from the proof of stability that $\bar{u}_m > \bar{z}/\beta$ is required. Hence, for a given $\bar{u}_m$ we can only guarantee that disturbances with relatively small magnitudes can be rejected. c) The condition on k is only sufficient, and, hence, the system can be stable even if Eq. (14) does not hold. This has been observed in numerous simulations. As k is increased beyond the bound defined in Eq. (14), but less than some critical upper bound, the control objective was still achieved even though the solutions of the system never entered the sliding regime. Hence a range of values for k exists for which the system will be stable without entering the sliding regime. However, this range of values for k turned out to be very difficult to compute analytically.

4) Even though the preceding control law is robust to uncertainty in J, prior knowledge of the bounds on the norm of J are required. This assumption will be relaxed in the adaptive variable structure controller presented in next section.

5) The disadvantages just mentioned are mainly a result of the use of a fixed value of k in the control law (13) and the strategy of attempting to stabilize both $\Omega(t)$ and $\epsilon(t)$ simultaneously from any initial condition. In practice, when the initial angular velocity $\Omega(0)$ of the spacecraft is large, the following strategy is commonly used: a detumbling control law is used to stabilize only $\Omega(t)$ first. After $\Omega(t)$ has been stabilized, another stabilizing control law is then used to bring both $\Omega(t)$ and $\epsilon(t)$ to zero. The same strategy can also be implemented using a combination of the control laws (12) and (13) and takes the form

$$u(t) = \begin{cases} -\Sigma\,[\Omega(t)]u_m & \text{if} \quad t \le \bar{t} \\ -\Sigma\,[s(t)]u_m & \text{otherwise} \end{cases} \quad (17)$$

where $\bar{t}$ is the time instant when $\Omega(t)$ reaches a small set around zero when controlled by $u(t) = -\Sigma\,[\Omega(t)]u_m$. We note that $\bar{t}$ is finite, which is a property guaranteed by the control law (12). When the control law (17) is used to stabilize the spacecraft, the conditions that need to be imposed on k and the disturbance in the proof of stability are less restrictive than those in the case when Eq. (13) is used. This is because the condition imposed on k in step 2 of the proof (see the Appendix) is directly related to the value of $\|\Omega(t)\|$ obtained after a finite time t_1 from any $\Omega(0)$. If $\|\Omega(t_1)\|$ is known to be small as a result of the use of $u(t) = -\Sigma\,[\Omega(t)]u_m$, then the condition on k can be relaxed accordingly, as there is no need to account for arbitrary large $\Omega(0)$ in step 1 of the proof.

VI.   Adaptive Variable Structure Controller

Another way to remove the drawbacks of the control law (13) is to adjust k adaptively. In this section we present one such adaptive VSC algorithm to ensure global stability and improve the response. We first recall that $s = \Omega + k\epsilon$ and suggest an adaptive variable structure controller in the form

$$u = -\Sigma\,(s)u_m \quad (18)$$

$$\dot{k} = -\gamma\,\bar{u}_m \sum_{i=1}^{3} [\text{sgn}(k)|\epsilon_i| + \epsilon_i\,\text{sgn}(s_i)] \quad (19)$$

where $u_m = [\bar{u}_m \ \ \bar{u}_m \ \ \bar{u}_m]^T$ and $\gamma > 0$ denotes the adaptive gain. This adaptive gain does not affect the stability analysis (as long as $\gamma > 0$) and can be chosen to improve the performance. We should emphasize that, despite adjusting the parameter k, the control inputs can still assume only their minimum and maximum values, i.e., $u(t) \in \mathcal{S}_u$ for all time.

Theorem 2: Under Assumption 1, all signals in the system (1–3), (5), (18), and (19) are bounded, and, in addition, $\lim_{t \to \infty} \Omega(t) = \lim_{t \to \infty} k(t)\epsilon(t) = 0$ for all $z \in \mathcal{S}_z$ and all $J = J^T > 0$.

Proof: Consider the Lyapunov function candidate

$$V(\Omega, k) = \tfrac{1}{2}[\Omega^T J\Omega + (1/\gamma)k^2]$$

The first derivative along the motion of Eqs. (1–3) is given by

$$\dot{V}(\Omega, k) = \Omega^T J\dot{\Omega} + \frac{1}{\gamma}k\dot{k}$$

$$= \Omega^T u + \Omega^T z - \sum_{i=1}^{3} \bar{u}_m k[\text{sgn}(k)|\epsilon_i| + \epsilon_i\,\text{sgn}(s_i)]$$

$$= (s - k\epsilon)^T[-\Sigma\,(s)u_m] + \Omega^T z$$

$$\quad - \sum_{i=1}^{3} \bar{u}_m[|k| \cdot |\epsilon_i| + k\epsilon_i\,\text{sgn}(s_i)]$$

$$= -\bar{u}_m \sum_{i=1}^{3} |s_i| + \Omega^T z - \sum_{i=1}^{3} \bar{u}_m|k\epsilon_i|$$

$$\le -(\bar{u}_m - \bar{z})\sum_{i=1}^{3}|s_i| - (\bar{u}_m - \bar{z})\sum_{i=1}^{3}|k\epsilon_i| \le 0$$

We used the fact that

$$\Omega^T z \le \|\Omega\|\bar{z} \le \|\Omega\|_1\bar{z} \le \bar{z}\left[\sum_{i=1}^{3}(|s_i| + |k\epsilon_i|)\right]$$

in arriving at the last inequality. Therefore, using the arguments from Ref. 23 it follows that $\Omega \in \mathcal{L}^\infty$ and $k \in \mathcal{L}^\infty$. Integrating $\dot{V}$ gives the result that $s \in \mathcal{L}^1$ and $k\epsilon \in \mathcal{L}^1$. Because $u \in \mathcal{L}^\infty$, it follows that ϵ, $\dot{\Omega}$, and hence $\dot{s}$ are all bounded. It is also noted that $\dot{k}$ is bounded as $\|\epsilon\|$ is bounded. Therefore $\lim_{t \to \infty} s(t) = \lim_{t \to \infty} k(t)\epsilon(t) = 0$, which implies that $\lim_{t \to \infty} \Omega(t) = 0$ as well. □

Based on the discussion just presented, we next include the following remarks:

1) Theorem 2 only guarantees that $k(t)\epsilon(t)$, but not necessarily $\epsilon(t)$, will converge to zero. If $k(t)$ converges to zero faster than $\epsilon(t)$, then $\epsilon(t)$ may converge to some nonzero constant value, as observed in simulation studies. To ensure that $\epsilon(t)$ will converge to zero, one needs to keep $k(t)$ from converging to zero. This can be achieved by using a sufficiently small γ such that $k(t)$ changes slowly and hence will not deviate too much from its initial value. We first note that $\dot{k}(t)$ is bounded below by $-6\gamma\,\bar{u}_m$. Hence $k(t) \ge k(0) - 6\gamma\,\bar{u}_m t$. Therefore, given a time interval for completing a certain maneuver, it is possible to choose a value of γ such that $k(t)$ is guaranteed to be larger than some desired value over the entire time interval.

2) The fact that $k(t)$ may tend to zero emphasizes the importance of condition (14). If $k(t)$ is small, the adaptation can be stopped at a value of $k(t)$ satisfying the condition (14). This assures the overall stability. In addition, $k(t)$ can be subsequently reset to a larger initial value to ensure sufficiently fast maneuvers.

3) This controller can also be modified to avoid chattering by using the approximate sign function in Eqs. (18) and (19). The effectiveness of the resulting controller is evaluated through simulations given in the next section.

4) Because the preceding design procedure does not guarantee that a sliding mode for the closed-loop system will exist, we refer to the preceding controller as the adaptive variable structure controller. The existence of a sliding mode is not needed to ensure global stability of the overall system.

5) Theorem 2 holds for all $J = J^T > 0$, which implies that the proposed control strategy is highly robust to large uncertainty in J. Furthermore, no information regarding J is needed to implement the controller. Hence the same controller can be used for different spacecraft without exact knowledge of their inertia matrices.

6) The proof for Theorem 2 can be readily extended to the case when $s = \Omega + k(\epsilon - \epsilon^*)$ and ϵ^* denotes some desired orientation. Hence the proposed controller is well suited for the case of point-to-point stabilization.

We can conclude that the adaptive controller (18) and (19) removes the already mentioned disadvantages of the control law (13) and results in a substantially simpler stability analysis. As shown in the following section, it also results in improved performance. All of this is a result of only a slight increase in the complexity of

the control law, i.e., when only one controller parameter is adjusted adaptively.

VII. Simulation

In this section we illustrate the effectiveness of the proposed control algorithms through numerical simulations. Because of space limitation, only figures that are essential for illustrating our results will be shown.

In the simulations we assumed that the nominal inertia matrix of the spacecraft is

$$J_N = \begin{bmatrix} 20 & 0 & 0.9 \\ 0 & 17 & 0 \\ 0.9 & 0 & 15 \end{bmatrix}$$

Further, the following initial conditions were chosen for all simulations: $\Omega(0) = [29 \ 29 \ 29]^T$ deg/s, $\epsilon(0) = [0.4 \ 0.2 \ 0.4]^T$, and $\epsilon_0(0) = 0.8$. The control authority is assumed to be $\bar{u}_m = 20$ Nm, and the disturbance is assumed to be bounded by $\bar{z} = 10$ Nm. The value of δ in the approximate sign function is set to 0.01 in all simulations.

We first note that the maximum and minimum eigenvalues of J_N are 20.2 and 14.8, respectively. Further, by choosing $\beta = 0.5$ in Eq. (14), we obtain 0.2 as the upper bound on k according to Theorem 1. Figure 3 shows the angular velocity of the spacecraft when the control law (16) is used to stabilize the system with $k = 0.2$. Even though $\Omega(t)$ appears to converge to zero, the response is too slow and may not be acceptable. Similar speed of response was also observed in $\epsilon(t)$. To improve the speed of response, we increased the value of k to 2.0. The resulting response is shown in Figs. 4 and 5. It is seen that both $\Omega(t)$ and $\epsilon(t)$ converge to zero in around 5 s. This illustrates the fact that the condition (14) on k is conservative. The same value of k (i.e., $k = 2.0$) is used in the next two simulations.

We tested the control law (16) in the presence of large input disturbance shown in Fig. 6 and found that the response is almost identical to that in the disturbance-free case shown in Figs. 4 and 5.
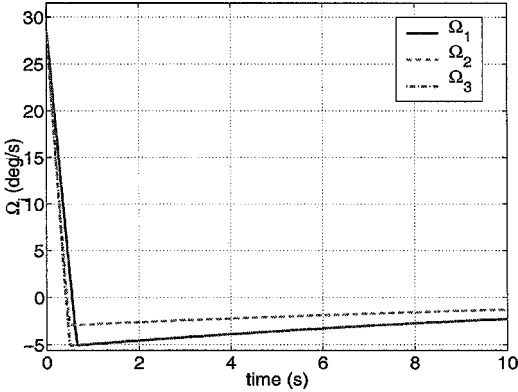

Fig. 3 Angular velocity $\Omega = [\Omega_1 \ \Omega_2 \ \Omega_3]^T$ under the control law (16): no disturbance case ($k = 0.2$).
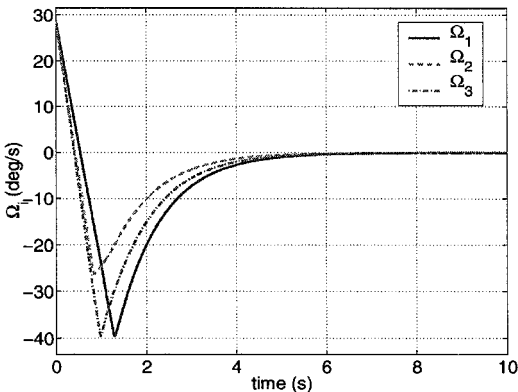

Fig. 4 Angular velocity $\Omega = [\Omega_1 \ \Omega_2 \ \Omega_3]^T$ under the control law (16): no disturbance case ($k = 2.0$).
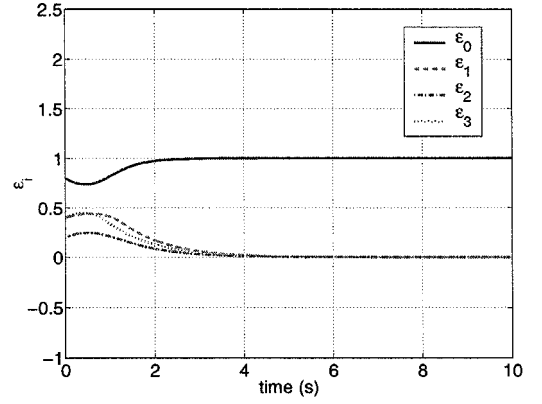

Fig. 5 Attitude $\epsilon = [\epsilon_0 \ \epsilon_1 \ \epsilon_2 \ \epsilon_3]^T$ under the control law (16): no disturbance case ($k = 2.0$).
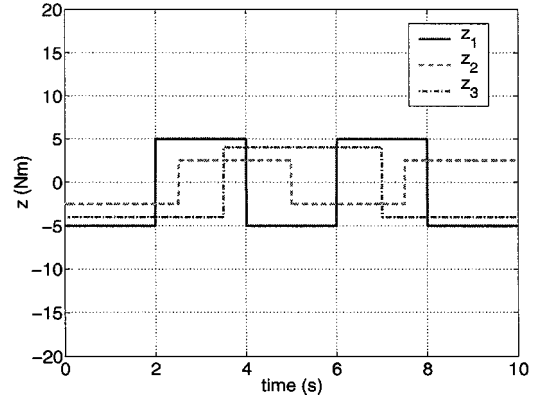

Fig. 6 External disturbance torque $z = [z_1 \ z_2 \ z_3]^T$.
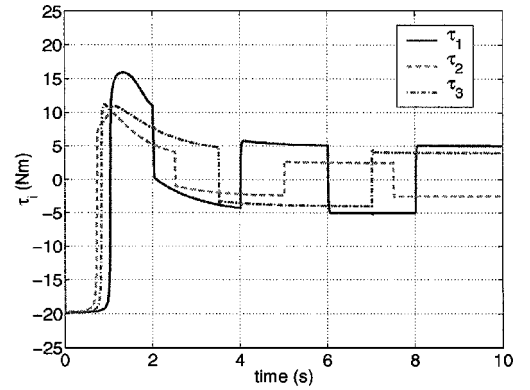

Fig. 7 Control torque $u = [\tau_1 \ \tau_2 \ \tau_3]^T$ under the control law (16): large external disturbance ($k = 2.0$).

The control torque is shown in Fig. 7, which indicates that the disturbance is effectively rejected by the control law (16). Because the disturbances are in the form of square waves, the control torques from Fig. 7 are bang-bang in nature, which can excite the flexible modes of the system. However, the designer has sufficient freedom to make the control torques slower by choosing sufficiently large δ. We also compared the performance of control law (8), with feedback terms in Ω and ϵ as suggested in Ref. 7, when control inputs are saturated under the same scenario. As expected, the response was essentially the same under this control law when the gains for the feedback terms in Ω and ϵ are sufficiently high. This is because the feedback terms will dominate the equivalent control terms, making the control law essentially the same as Eq. (16). The main difference between the two algorithms is that in this paper global stability under input saturation is proved explicitly for the control laws (16), (18), and (19), whereas there is no such result for the control law from Ref. 7 with saturated inputs.

The control law (16) was also tested on another spacecraft model with the inertia matrix equal to $1.25J_N$. The control objective is still achieved despite such large change in inertia matrix, as the control law (16) is independent of J. We should also emphasize that in all simulations the response is free of chattering as a result of the use of the approximate sign function.

We next carried out simulations to illustrate the effectiveness of the adaptive control law (18) and (19). As in the preceding case, in all simulations we used the approximate sign function in the control law to avoid chattering of the control input. The value of k was initialized at 2.0. Figures 8 and 9 show the angular velocity and attitude of the spacecraft respectively when the control law (18) and (19) with $\gamma = 0.01$ was used to stabilize the system. It is seen that the control objective is achieved and $k(t)$ converges to around 1.4 (Fig. 10). The control law (18) and (19) was also tested for the same disturbances and the same change in inertia matrix as in the case of control law (16), as well as when both these uncertainties plus mea-
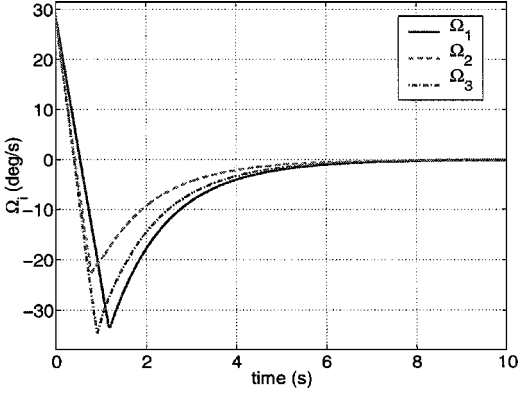

Fig. 8   Angular velocity $\Omega = [\Omega_1\ \Omega_2\ \Omega_3]^T$ under the control law (18) and (19): no disturbance case.
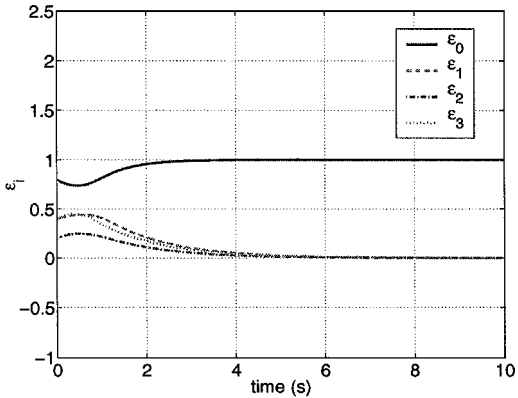

Fig. 9   Attitude $\epsilon = [\epsilon_0\ \epsilon_1\ \epsilon_2\ \epsilon_3]^T$ under the control law (18) and (19): no disturbance case.
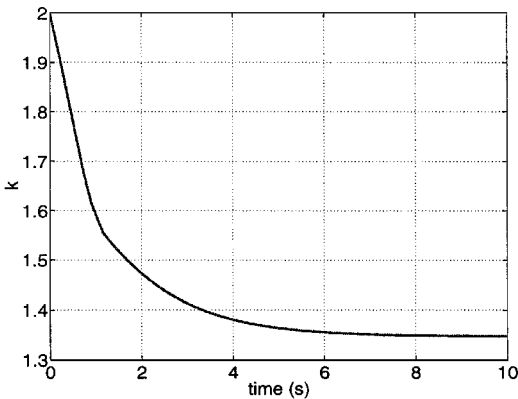

Fig. 10   Adaptive parameter k.

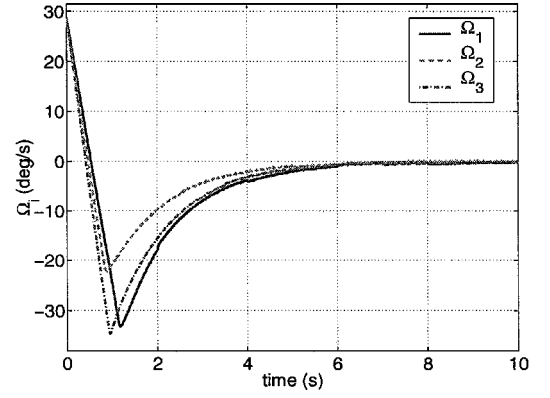Fig. 11   Angular velocity $\Omega = [\Omega_1\ \Omega_2\ \Omega_3]^T$ under the control law (18) and (19): external disturbances, measurement noise, inertia matrix $J = 1.25J_N$.
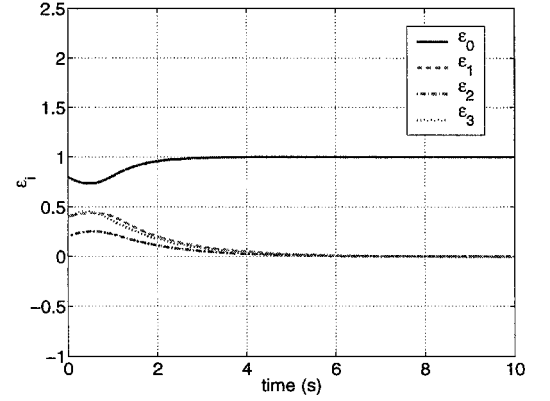

Fig. 12   Attitude $\epsilon = [\epsilon_0\ \epsilon_1\ \epsilon_2\ \epsilon_3]^T$ under the control law (18) and (19): external disturbances, measurement noise, inertia matrix $J = 1.25J_N$.

surement noise are present simultaneously. The response is excellent in all cases. Because of space limitation, we only show the response of the spacecraft in the last case (Figs. 11 and 12). The measurement noise present in this simulation is of magnitude 0.1 deg/s in the angular velocities and 0.001 in the quaternions. Even though the magnitude of noise is unrealistically large, the performance is virtually nondistinguishable from that obtained in the case when there is no uncertainty (Figs. 8 and 9). This illustrates the robustness of the control law (18) and (19) to the simultaneous presence of different types of uncertainties and disturbances. Because of the large noise, the control input computed by the algorithm (18) and (19) is fairly oscillatory. However, in practice, the actual input torque is filtered by the actuator dynamics. A larger initial condition $k(0)$ results in a faster convergence of $\epsilon(t)$ to zero. Hence the designer has sufficient freedom to achieve the desired weighting between the speed of response of $\Omega(t)$ and $\epsilon(t)$.

VIII.   Conclusion

In this paper we propose two control algorithms based on variable structure control for spacecraft stabilization in the presence of parametric uncertainty, bounded external disturbances, and control input saturation. The first algorithm is based on the variable structure component of the standard sliding mode control law for spacecraft stabilization. We also propose an adaptive version of this algorithm that removes the disadvantages of the sliding mode controller and results in improved response in the presence of disturbances and large parametric uncertainty. In both cases we included rigorous proof of stability of the resulting closed-loop system, as well as computer simulations to evaluate the overall performance.

The main contribution of the paper is that the proposed control laws for spacecraft ensure that the control objective is achieved with limited control authority. The control laws are simple to implement and are demonstrated to be effective in compensating for large parametric uncertainty and bounded disturbances.

Our future research directions include the following: 1) extensions of the proposed algorithms to the case of tracking (some preliminary simulation have revealed that this is a viable approach, and the related stability analysis is currently in progress); 2) use of these algorithms as baseline control laws for spacecraft failure detection and identification and adaptive reconfigurable control; and 3) combination of these algorithms with on-line nonlinear estimators to achieve fast and accurate rejection of state-dependent disturbances.

Appendix: Proof of Theorem 1

The proof of Theorem 1 consists of three main steps. We will give the details of the first two steps here. The last step of the proof is the same as in the case of equivalent control-based sliding mode controller design for spacecraft described in Sec. IV.

Our overall objective is to demonstrate that the motion of the closed-loop system starting from any initial condition enters a compact set containing the origin in finite time. Following that, the motion of the system reaches the sliding surface, also in finite time. Once the sliding surface is reached, the system enters into the sliding regime as described in Sec. IV so that both $\Omega(t)$ and $\epsilon(t)$ converge to zero. The finite time response requirement in the first two steps is important to demonstrate the overall asymptotic stability of the system.

Step 1: The objective in this step is to prove that there exists a scalar $\bar{\Omega} > 0$ such that any motion of $\Omega(t)$ starting from an arbitrary $\Omega(0)$ will enter a closed compact set $\mathcal{P} \triangleq \{\Omega : \|\Omega\| \le \bar{\Omega}\}$ in finite time. To demonstrate this, we start our analysis by choosing

$$V_1(\Omega) = \tfrac{1}{2}\Omega^T J \Omega$$

We will show that $\dot{V}_1(\Omega) \le -\alpha_1\|\Omega\|$, for some $\alpha_1 > 0$, when $\Omega \in \mathcal{P}^c$, where $\mathcal{P}^c$ denotes the complement of $\mathcal{P}$. This implies that there exists an $\bar{\alpha}_1 > 0$ such that $\dot{V}_1 \le -\bar{\alpha}_1\sqrt{V_1}$. By integrating this inequality, we can conclude that the set $\mathcal{P}$ will be reached in finite time. The details of this argument are given next.

The first derivative of $V_1(\Omega)$ along the motion of Eq. (1) is given by

$$\dot{V}_1(\Omega) = \Omega^T J \dot{\Omega}$$
$$= \Omega^T u + \Omega^T z$$
$$= -\sum_{i=1}^{3} \bar{u}_m \Omega_i \operatorname{sgn}(s_i) + \Omega^T z$$

By statement 1) of Assertion 1, if $|\Omega_i| > k$ for $i = 1, 2, 3$, then

$$\Omega_i \operatorname{sgn}(s_i) = \Omega_i \operatorname{sgn}(\Omega_i) = |\Omega_i|$$

$$\dot{V}_1(\Omega) \le -\sum_{i=1}^{3} |\Omega_i|\bar{u}_m + \|\Omega\|\bar{z} \le -(\bar{u}_m - \bar{z})\|\Omega\| < 0$$

under Assumption 1. However, $|\Omega_i| > k$ for $i = 1, 2, 3$ simultaneously is not true in general, and one has to determine a set $\mathcal{P}$ such that $\dot{V}_1(\Omega) \le -\alpha_1\|\Omega\|$ when $\Omega \in \mathcal{P}^c$, even if $|\Omega_i| \le k$ for some i. The strategy adopted here is to find a set $\mathcal{P}$ sufficiently large such that at least one term in $\dot{V}_1(\Omega)$ is negative and has magnitude large enough to cover the other sign-indefinite terms in that expression.

Consider the cube $\mathcal{C} \triangleq \{\Omega : |\Omega_i| \le k, \ i = 1, 2, 3\}$ in the Ω space. If $\Omega \in \mathcal{C}^c$, then $|\Omega_j| > k$ for at least one j. Because we are interested in expressing the condition on Ω in terms of its norm, we consider the set $\bar{\mathcal{P}} \triangleq \{\Omega : \|\Omega\| \le \sqrt{(3)}k\}$, which is the smallest ball containing the set $\mathcal{C}$. Therefore, $\Omega \in \bar{\mathcal{P}}^c$ implies that $\Omega \in \mathcal{C}^c$, which in turn implies that $|\Omega_j| > k$ for at least one j. In such a case we have

$$\dot{V}_1(\Omega) \le -\bar{u}_m \Omega_j \operatorname{sgn}(\Omega_j) - \bar{u}_m \sum_{i=1, i\neq j}^{3} \Omega_i \operatorname{sgn}(s_i) + \Omega^T z$$

$$= -\bar{u}_m |\Omega_j| - \bar{u}_m \sum_{i=1, i\neq j}^{3} \Omega_i \operatorname{sgn}(s_i) + \Omega^T z \quad \text{for} \quad \Omega \in \bar{\mathcal{P}}^c$$

By statement 2) of Assertion 1, we can get an upper bound for the second term in the preceding expression, which yields

$$\dot{V}_1(\Omega) \le -\bar{u}_m\left[|\Omega_j| + \sum_{i=1, i\neq j}^{3} (|\Omega_i| - 2k)\right] + \Omega^T z$$

$$\text{for} \quad \Omega \in \bar{\mathcal{P}}^c$$

We can now rewrite the preceding expression in the form

$$\dot{V}_1(\Omega) \le -\bar{u}_m\left(\sum_{i=1}^{3} |\Omega_i| - 4k\right) + \Omega^T z$$

$$\le -\bar{u}_m(\|\Omega\| - 4k) + \Omega^T z$$

$$\text{for} \quad \Omega \in \bar{\mathcal{P}}^c (\text{because } \|\Omega\| \le \|\Omega\|_1)$$

Because $\Omega \in \bar{\mathcal{P}}^c$ is not sufficient to conclude that $\dot{V}_1(\Omega) < 0$, we next consider the set $\mathcal{P} \triangleq \{\Omega : \|\Omega\| \le 4k/(1-\beta)\}$ for some $0 < \beta < 1$. If $\Omega \in \mathcal{P}^c$, then the condition imposed earlier that $\Omega \in \bar{\mathcal{P}}^c$ is still valid as $\mathcal{P}^c \subset \bar{\mathcal{P}}^c$ [because $4k/(1-\beta) \ge 4k > \sqrt{(3)}k$]. Furthermore, we have $4k \le (1-\beta)\|\Omega\|$, which implies

$$\dot{V}_1(\Omega) \le -\bar{u}_m(\|\Omega\| - (1-\beta)\|\Omega\|) + \Omega^T z$$

$$= -\bar{u}_m \beta\|\Omega\| + \Omega^T z \qquad \text{for} \qquad \Omega \in \mathcal{P}^c$$

Because $\|z\|$ is bounded by $\bar{z}$, we have

$$\dot{V}_1(\Omega) \le -(\bar{u}_m\beta - \bar{z})\|\Omega\|$$

Hence

$$\dot{V}_1(\Omega) < 0 \qquad \text{for} \qquad \Omega \in \mathcal{P}^c, \qquad \bar{u}_m > \bar{z}/\beta$$

Because $V_1(\Omega) \le \tfrac{1}{2}\bar{\lambda}_J\|\Omega\|^2$, $\dot{V}_1 \le -(\bar{u}_m\beta - \bar{z})\sqrt{(2/\bar{\lambda}_J)}\sqrt{V_1}$, and $\sqrt{V_1(t)} \le \{\sqrt{[V_1(0)]} - [1/\sqrt{(2\bar{\lambda}_J)}](\bar{u}_m\beta - \bar{z})t\}^2$ as long as $\Omega \in \mathcal{P}^c$ and $\bar{z} < \bar{u}_m\beta$. This means $\Omega(t)$ will reach the ball $\mathcal{P}$ in finite time.

The smaller the value of β is, then the disturbance that can be rejected for a given control authority is also smaller in this analysis. However, the value of β also has an effect on how large k can be, as we will show in the next step of the proof. Therefore the choice of β is a compromise between the disturbance rejection capability of the controller and the freedom of choosing k.

Step 2: Consider another scalar function

$$V_2(s) = \tfrac{1}{2}s^T J s$$

Its first derivative along the motion of Eqs. (1–3) yields

$$\dot{V}_2(s) = s^T J \dot{s}$$
$$= ks^T\left[\epsilon^\times J + \tfrac{1}{2}J(\epsilon^\times + \epsilon_0 I)\right]\Omega + s^T u + s^T z$$
$$\le k\left(\|\epsilon^\times\| + \tfrac{1}{2}\|\epsilon^\times + \epsilon_0 I\|\right)\|J\| \cdot \|s\| \cdot \|\Omega\|$$
$$+ s^T u + s^T z$$

where $\|\epsilon^\times\|$, $\|\epsilon^\times + \epsilon_0 I\|$ and $\|J\|$ are the induced norm of the respective matrices. It can be readily shown that $\|\epsilon^\times\| \le 1$ and $\|\epsilon^\times + \epsilon_0 I\| \le 1$. Recall that $\bar{\lambda}_J$ is defined as the upper bound of the norm of the inertia matrix J. Therefore,

$$\dot{V}_2(s) \le \frac{3}{2}\bar{\lambda}_J k\|s\| \cdot \|\Omega\| - \bar{u}_m \sum_{i=1}^{3} |s_i| + s^T z$$

$$\le \frac{3}{2}\bar{\lambda}_J k\|s\| \cdot \|\Omega\| - \bar{u}_m\|s\| + s^T z \quad (\text{because } \|s\| \le \|s\|_1)$$

From step 1 we know that $\Omega(t)$ will enter $\mathcal{P}$ in finite time. Suppose $\Omega(t)$ reaches $\mathcal{P}$ at $t = t_1$ [$t_1 = 0$ if $\Omega(0) \in \mathcal{P}$]. Because $\dot{V}_1(\Omega) < 0$

for $\Omega \in \mathcal{P}^c$, it can be easily verified that $\|\Omega(t)\| \le 4k\bar{\lambda}_J / [(1-\beta)\underline{\lambda}_J]$ for $t > t_1$. Then we have

$$\dot{V}_2(s) \le \left\{ [6/(1-\beta)\underline{\lambda}_J]\bar{\lambda}_J^2 k^2 - \bar{u}_m + \bar{z} \right\} \|s\| \quad \text{(because } \|z\| < \bar{z})$$

$$\text{for} \quad \Omega \in \mathcal{P}$$

Hence, if

$$k < \sqrt{(1-\beta)(\bar{u}_m - \bar{z})\underline{\lambda}_J \big| 6\bar{\lambda}_J^2}$$

then $\dot{V}_2(s) < 0$ for $t < t_1$. Using the fact that $V_2(s) \le \frac{1}{2}\bar{\lambda}_J \|s\|^2$, it can be shown that $\dot{V}_2 \le -\bar{a}\sqrt{V_2}$ for some $\bar{a} > 0$. Hence it can be readily shown that $\|s(t)\| \le a - b(t - t_1)$, for some $a, b > 0$ and $t \in (t_1, t_1 + a/b]$. This implies that $s = 0$ is reached in finite time. □

Acknowledgments

References

[1]Wang, P. K. C., and Hadaegh, F. Y., "Coordination and Control of Multiple Microspacecraft Moving in Formation," *Journal of Astronautical Sciences*, Vol. 44, No. 3, 1996, pp. 315–355.

[2]Wang, P. K. C., Hadaegh, F. Y., and Lau, K., "Synchronized Formation Rotation and Attitude Control of Multiple Free-Flying Spacecraft," *Journal of Guidance, Control, and Dynamics*, Vol. 22, No. 1, 1999, pp. 28–35.

[3]Singh, S. A., "Robust Nonlinear Attitude Control of Flexible Spacecraft," *IEEE Transactions on Aerospace and Electronic Systems*, Vol. AES-23, No. 3, 1987, pp. 380–387.

[4]Hughes, P. C., *Spacecraft Attitude Dynamics*, Wiley, New York, 1986, Chap. 2, pp. 6–31.

[5]Wen, J. T.-Y., and Kreutz-Delgado, K., "The Attitude Control Problem," *IEEE Transactions on Automatic Control*, Vol. 36, No. 10, 1991, pp. 1148–1162.

[6]Ahmed, J., Coppola, V. T., and Bernstein, D. S., "Adaptive Asymptotic Tracking of Spacecraft Attitude Motion with Inertia Matrix Identification," *Journal of Guidance, Control, and Dynamics*, Vol. 21, No. 5, 1998, pp. 684–691.

[7]Robinett, R. D., Parker, G. P., Schaub, H., and Junkins, J. L., "Lyapunov Optimal Saturated Control for Nonlinear Systems," *Journal of Guidance, Control, and Dynamics*, Vol. 20, No. 6, 1997, pp. 1083–1088.

[8]Emelyanov, S. V., *Variable Structure Control Systems*, Nauka, Moscow, 1967 (in Russian).

[9]Utkin, V. I., "Variable Structure Systems with Sliding Modes," *IEEE Transactions on Automatic Control*, Vol. 22, No. 2, 1997, pp. 212–222.

[10]DeCarlo, R. A., Zak, S. H., and Matthews, G. P., "Variable Structure Control of Nonlinear Multivariable Systems: A Tutorial," *Proceedings of the IEEE*, Vol. 76, No. 3, 1988, pp. 212–232.

[11]Hung, J. Y., Gao, W., and Hung, J. C., "Variable Structure Control: A Survey," *IEEE Transactions on Industrial Electronics*, Vol. 40, No. 1, 1993, pp. 2–22.

[12]Bošković, J. D., "A Multiple Model-Based Controller for Nonlinearly-Parametrized Plants," *Proceedings of the American Control Conference*, American Automatic Control Council, Evanston, IL, 1997, pp. 2140–2144.

[13]Narendra, K. S., and Bošković, J. D., "Robust Adaptive Control Using a Combined Approach," *International Journal of Adaptive Control and Signal Processing*, Vol. 4, No. 2, 1990, pp. 111–131.

[14]Narendra, K. S., and Bošković, J. D., "A Combined Direct, Indirect and Variable Structure Method for Robust Adaptive Control," *IEEE Transactions on Automatic Control*, Vol. 37, No. 2, 1992, pp. 262–268.

[15]Singh, S. A., and Iyer, A., "Nonlinear Decoupling Sliding Mode Control and Attitude Control of Spacecraft," *IEEE Transactions on Aerospace and Electronic Systems*, Vol. 25, No. 5, 1989, pp. 621–633.

[16]Dwyer, T. A. W., III, and Sira-Ramirez, H., "Variable-Structure Control of Spacecraft Attitude Maneuvers," *Journal of Guidance, Control, and Dynamics*, Vol. 11, No. 3, 1988, pp. 262–270.

[17]Crassidis, J. L., and Markley, F. L., "Sliding Mode Control Using Modified Rodrigues Parameters," *Journal of Guidance, Control, and Dynamics*, Vol. 19, No. 6, 1996, pp. 1381–1383.

[18]Lo, S.-C., and Chen, Y.-P., "Smooth Sliding-Mode Control for Spacecraft Attitude Tracking Maneuvers," *Journal of Guidance, Control, and Dynamics*, Vol. 18, No. 6, 1995, pp. 1345–1349.

[19]McDuffie, J. H., and Shtessel, Y. B., "A Sliding Mode Controller and Observer for Satellite Attitude Control," *AIAA Guidance, Navigation, and Control Conference*, AIAA, Reston, VA, 1997, pp. 1613–1619.

[20]Vadali, S. R., "Variable-Structure Control of Spacecraft Large-Angle Maneuvers," *Journal of Guidance, Control, and Dynamics*, Vol. 9, No. 2, 1986, pp. 235–239.

[21]Terui, F., "Position and Attitude Control of a Spacecraft by Sliding Mode Control," *Proceedings of the American Control Conference*, American Automatic Control Council, Evanston, IL, 1998, pp. 217–221.

[22]Yoshizava, T., "Stability Theory by Liapunov's Second Method," *The Mathematical Society of Japan*, Tokyo, 1966.

[23]Narendra, K. S., and Annaswamy, A. M., *Stable Adaptive Systems*, Prentice–Hall, Upper Saddle River, NJ, 1989, Chap. 3, pp. 99–136.